Electron Density Distribution Analysis for Nitromethane, Nitromethide, and Nitramide[†]

James P. Ritchie

*Contribution from Los Alamos National Laboratory, Los Alamos, New Mexico 87545.
Received July 23, 1984*

Abstract: Electron density distributions for nitromethane, nitramide, and nitromethide were calculated by a procedure that is a simple variation of Streitwieser's algorithm used for evaluating the projected electron density in a single plane. This modified procedure allows quantitative electron populations to be obtained for any arbitrary three-dimensional region of the molecule. Additionally, the volume, surface area, and dimensions associated with given constant electron density surfaces are presented. Using the same computational procedure, spherically averaged electron distributions for isolated atoms were generated. When these charge distributions are placed at the appropriate nuclear coordinates of the molecule's constituent atoms and their sum evaluated on a grid, a distribution is generated of the so-called promolecule. This distribution is then subtracted from the molecular distribution to form density deformation maps (DDM's). The DDM's for nitromethane, nitromethide, and nitramide were calculated; positive deformations were observed along C–H, N–H, and C–N bonds and in regions corresponding to lone pairs of electrons; negative deformations were observed along O–N and N–N bonds and at the heavy-atom nuclei. Finally, atom-centered multipole expansions were obtained directly from the electron distributions as suggested by Hirshfeld and used to calculate the electrostatic potential. This procedure works well, provided that the atoms of the molecule are not approached too closely, and can be carried out quickly enough to allow three-dimensional potentials to be calculated once the multipole expansions have been obtained.

This paper examines the electron density distribution as determined by a novel technique from ab initio self-consistent-field calculations for the 32 electron molecules nitromethane (CH_3NO_2), nitromethide ($CH_2NO_2^-$), and nitramide (NH_2NO_2). These molecules were chosen because of the interest in their reactions from the standpoint of rate–equilibrium relationships and because they contain three groups commonly found in explosives: the nitro group, as in nitrated hydrocarbons and benzenes; a charge-carrying nitro group, as in picrates; and a nitramine group, as in RDX and HMX (hexahydro-1,3,5-trinitro-*s*-triazine and octahydro-1,3,5,7-tetranitro-1,3,5,7-tetrazocine). Consequently, insight into their electronic structure may lead to a better understanding of their reactions and properties.

The method used here of calculating the electron density at a point is based upon Streitwieser's procedure whereby electron densities are projected into a single plane so as to allow the quantitative calculation of electron populations contained within arbitrary regions of the plane.[1] A slight variation of his original procedure allows the efficient calculation of electron densities on a three-dimensional grid and the quantitative integration of electron densities to produce electron populations contained within completely arbitrary three-dimensional surfaces. Furthermore, the volume, surface area, and distance of closest approach to the molecule's atoms associated with a constant electron density surface are calculated, along with the enclosed electron population. The indexes obtained in this fashion are compared with other more standard indexes.[2]

Electron density is next apportioned among the atoms of the molecule according to the Hirshfeld criterion.[3] This method is implemented by first constructing a so-called promolecule, which is formed by the superposition of spherically averaged atomic densities obtained from the current procedure. Density from the molecule is then assigned to each atom in the molecule in the same proportion as the atom contributes charge to the promolecule.

Following Hirshfeld,[3] atom-centered multipole expansions are next obtained from which the molecular electrostatic potential is calculated. The potential thus obtained is shown to approximate rigorous calculations for nitromethane, nitromethide, and nitramide.

Methods

Self-consistent-field calculations and geometry optimizations were performed with the program HONDO5[4] with the 3-21G basis set throughout.[5] The 3-21G basis set seems to provide a reasonable compromise between accuracy and expense for the current purposes, while it is small enough to be used in the study of significantly larger molecules in the future. Further programs to perform electron density distribution analysis calculations are currently running on a Cray as stand-alone programs which take the same input as HONDO; nevertheless, it would be an easy matter to integrate these programs as subroutines in HONDO.[6]

Electron Densities. The total electron density at a point is given in eq 1, where i and j run over basis functions, P_{ij} is a density

$$\rho(x,y,z) = \sum_i \sum_j P_{ij} \phi_i(x,y,z) \phi_j(x,y,z) \tag{1}$$

matrix element, and $\phi_i(x,y,z)$ is the value of basis function i at x,y,z. In this form, eq 1 can be integrated over finite regions only with difficulty to yield electron populations of quantitative accuracy. This is due in large part to the highly spiked character of the electron density function at the nuclei.

Streitwieser et al.,[1] however, pointed out that if the summation indexes are allowed to run over the uncontracted Gaussian primitive functions that form the basis functions, rather than basis functions themselves, a separation of variables was possible, leading to eq 2

$$\rho(x,y,z) = \sum_k \sum_l P'_{kl} FX_{kl}(x) FY_{kl}(y) FZ_{kl}(z) \tag{2}$$

where

(1) (a) Collins, J. B.; Streitwieser, A., Jr.; McKelvey, J. M. *Comput. Chem.* **1979**, *3*, 79–81. (b) Streitwieser, A., Jr.; Grier, D. L.; Kohler, B. A. B.; Vorpagel, E. R.; Schriver, G. W. In "Electron Distributions and the Chemical Bond"; Coppens, P., Hall, M. B., Eds.; Plenum Press: New York, 1982; pp 447–473.

(2) See, for example: (a) Gavezotti, A. *J. Am. Chem. Soc.* **1983**, *105*, 5220–5225. (b) Gavezotti, A. *Nouv. J. Chim.* **1982**, *6*, 443–450. (c) Bondi, A. *J. Phys. Chem.* **1964**, *68*, 441–451.
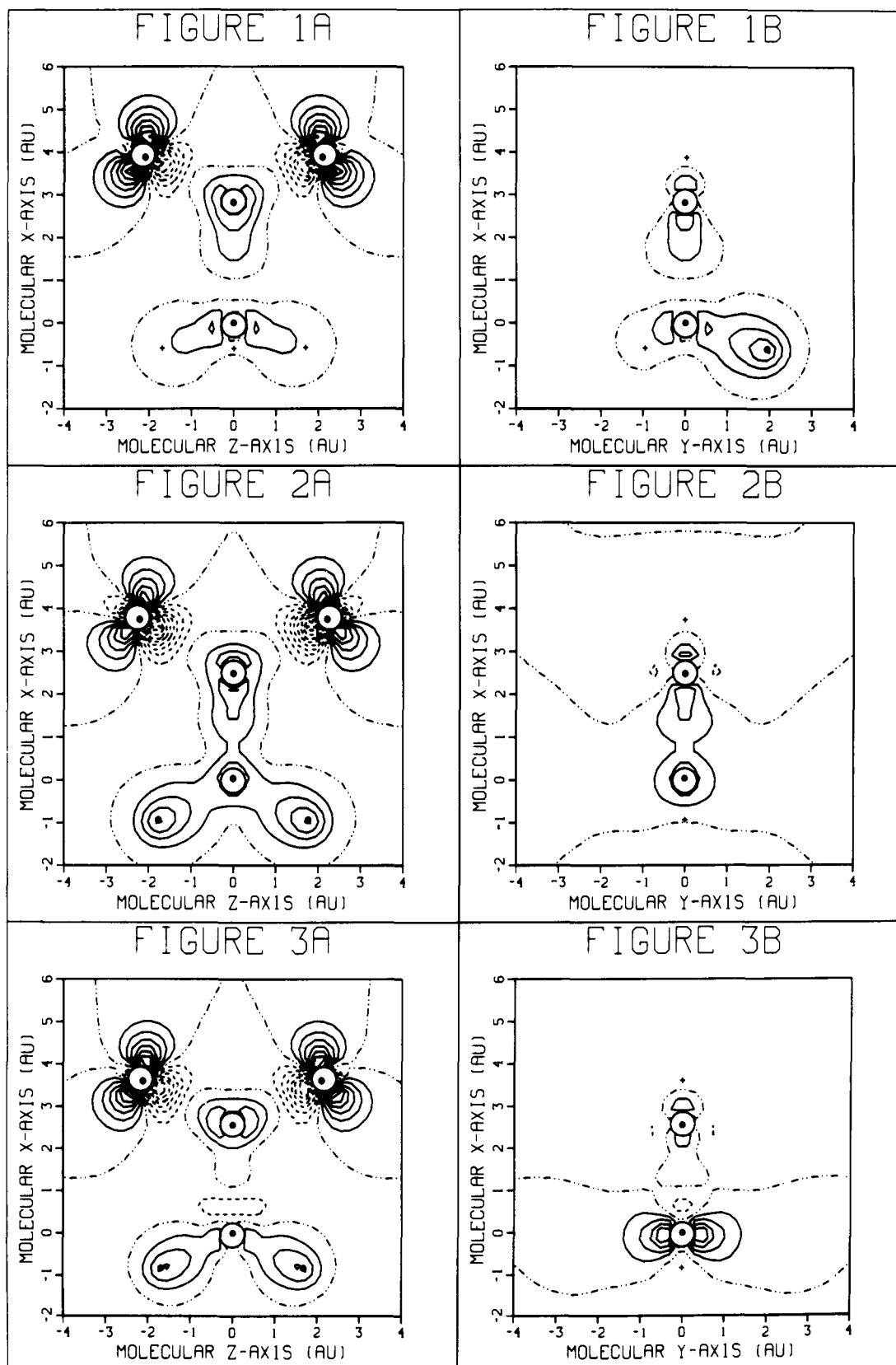
(3) Hirshfeld, F. L. *Theor. Chim. Acta* **1977**, *49*, 129–138.

(4) Dupuis, M.; Rys, J.; King, H. F. "Quantum Chemistry Program Exchange", Indiana University, Bloomington, IN, No. 401.

(5) Binkley, J. S.; Pople, J. A.; Hehre, W. J. *J. Am. Chem. Soc.* **1980**, *102*, 939–947.

(6) The programs described in this paper will be available from the author upon written request accompanied by a magnetic tape.

Figures 1–3. Calculated density deformation maps in e/au^3 for nitromethane (Figure 1), nitromethide (Figure 2), and nitramide (Figure 3) in the plane containing all heavy atoms (A) and in the perpendicular symmetry plane (B). Solid lines correspond with positive values, dashed lines correspond with negative values, and the combination dash-dot lines correspond with zero as a value. Contours are drawn each 0.04 e/au^3. Positions of atoms that are in the illustrated plane are marked by a heavy dot (•) and projections of atoms into the plane are indicated by a plus sign (+). Regions within 0.15 Å of the heavy atoms are blanked out to emphasize the positions of the atoms.

P'_{kl} = density matrix element appropriate for uncontracted
Gaussian primitives k and l

$$FX_{kl}(q) = GX_k(q)GX_l(q) \qquad (3)$$

$$GX_k(q) = \text{sign}(a_k)|a_k|^{1/3}(q - X_0)^{n_{x,k}} \exp\{-\alpha_k(q - X_0)^2\} \qquad (4)$$

In eq 4, a_k is the contraction coefficient, $n_{x,k}$ is the Cartesian exponent, and α_k is the Gaussian exponent associated with the
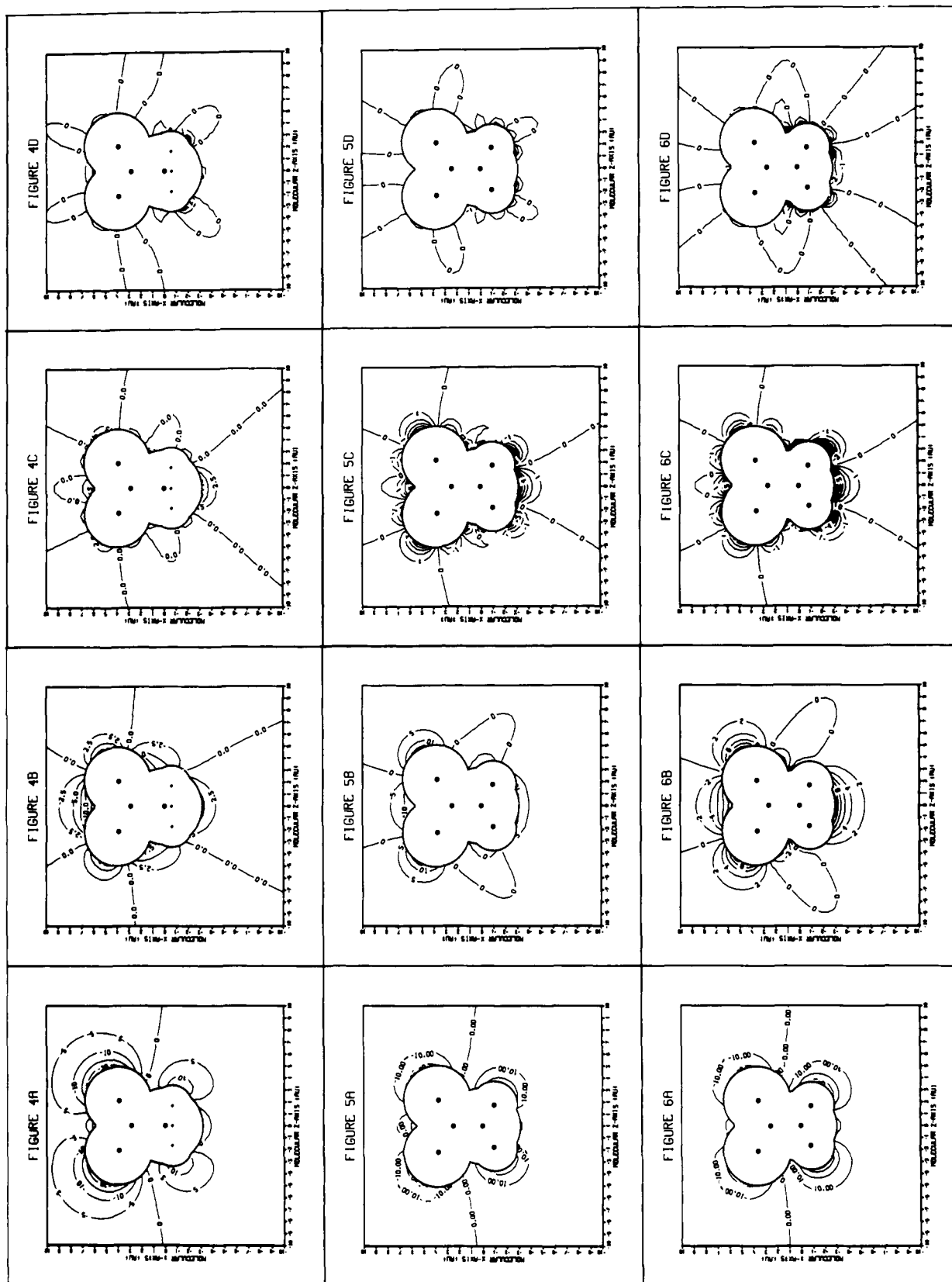
Figures 4–6. Contributions of dipoles (A), quadrupoles (B), octopoles (C), and hexadecapoles (D) to the electric potential in kcal e^{-1} for nitromethane (Figure 4), nitromethide (Figure 5), and nitramide (Figure 6) in the plane of the heavy atoms. Atom positions in the plane illustrated are marked by a heavy dot ($\bullet$), while positions of atoms projected into the plane are marked by a plus sign (+). For clarity, contour values are labeled where possible, but they always occur at a constant increment in any one figure. Contours are drawn in Figures 4D–6D at 1 kcal e^{-1}. Regions within a van der Waals radius of an atom are blanked out.

X component of the kth Gaussian function centered at X_0. The FY and FZ functions represent the y and z components analogous to those specified in eq 3 and 4 for the x components.

At this point, if the electron density is to be projected into a single plane, integration can be performed over one of the three Cartesian coordinates.[1] For the present purpose, however, no integration is performed and the above procedure can be modified[1] to yield accurate electron populations by averaging $FX_{kl}(q)$ in
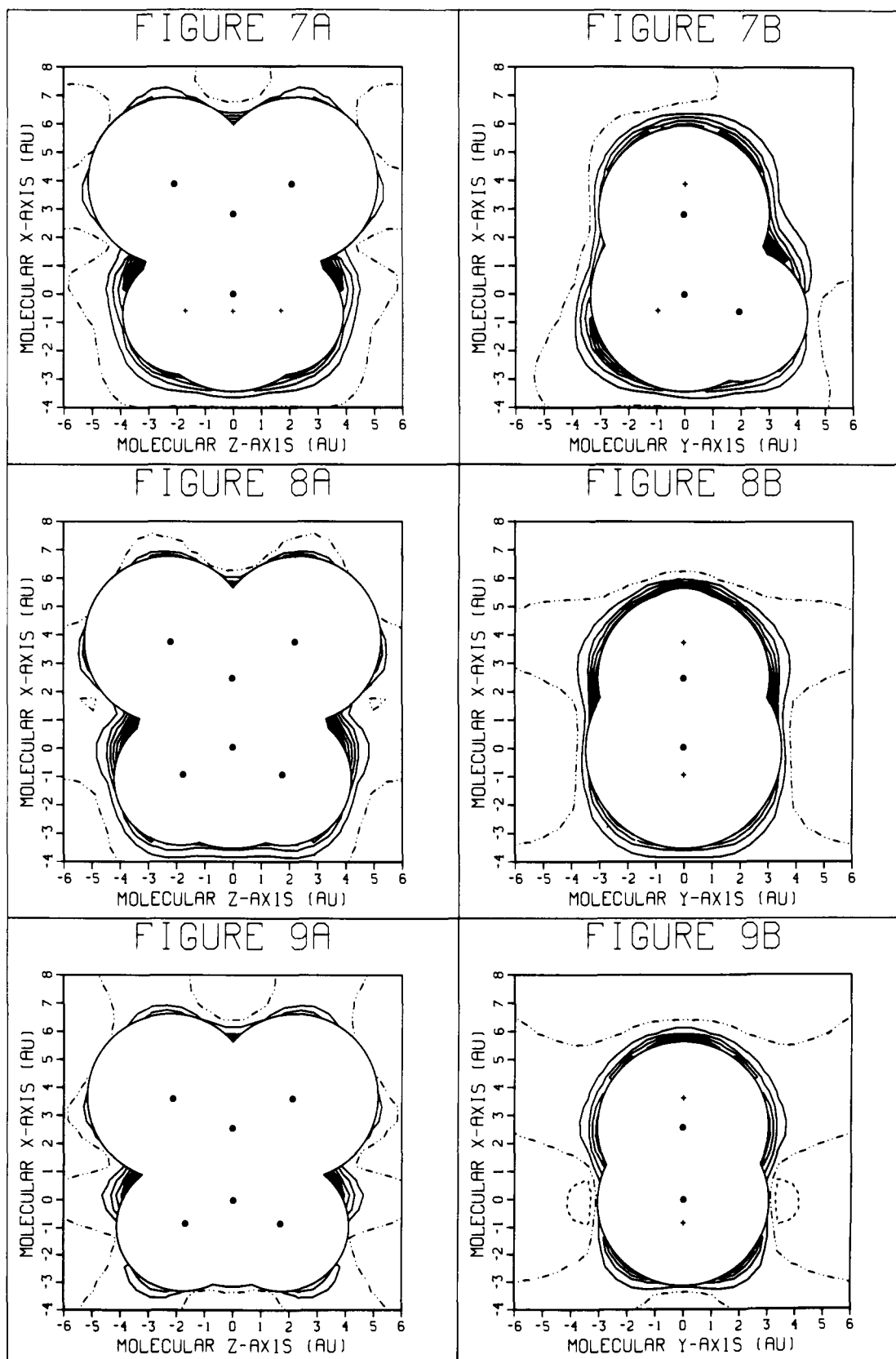
Figures 7-9. Electrostatic potential calculated rigorously minus that calculated from multipole expansions in kcal e^{-1} for nitromethane(Figure 7), nitromethide (Figure 8), and nitramide (Figure 9). Planes are those including the heavy atoms (A) and in the perpendicular symmetry plane (B). Positions of atoms in the plane are marked by a heavy circle (•), while projected atom positions are marked with a plus sign (+). Regions within which the multipole expansions give large errors are blanked and are determined from the van der Waals radii of the atoms.[2c] Contours appear as in Figures 1-3 at an interval of 1 kcal e^{-1}.
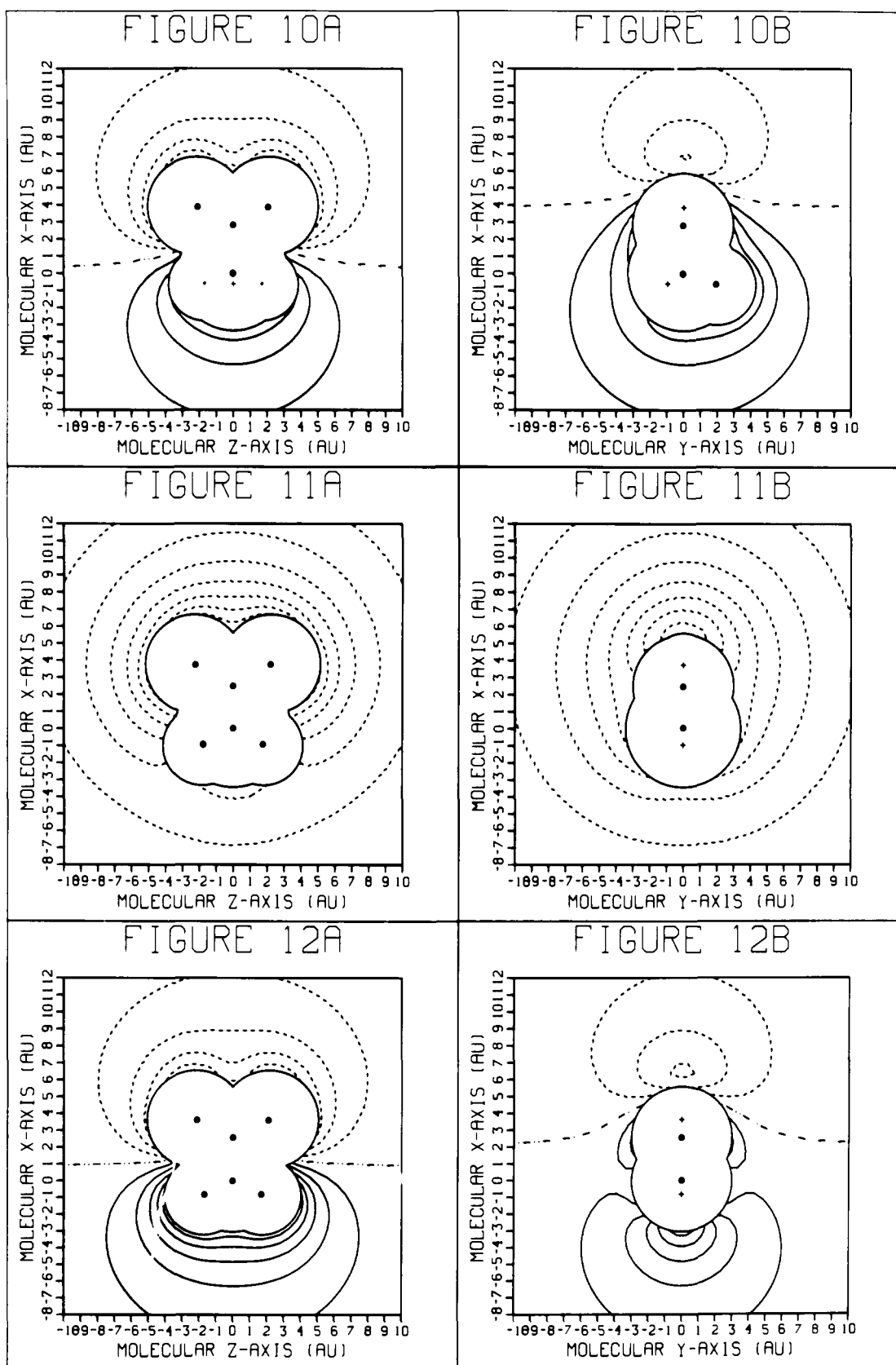
Figures 10–12. Electrostatic potential from multipole expansions in kcal e⁻¹ for nitromethane (Figure 10), nitromethide(Figure 11), and nitramide (Figure 12) in the plane of the heavy atoms (A) and the perpendicular symmetry plane (B). Positions of atoms in the planes are marked by a heavy circle (•), while projected positions of atoms not in the plane are marked with a plus sign (+). Regions within which the multipole expansions give large errors are blanked and are determined from standard van der Waals radii of the atoms. Contours appear as in Figures 1–3, at an interval of 10 kcal e⁻¹ for Figures 10 and 12 and 20 kcal e⁻¹ for Figure 11. The outermost contour in Figure 11 has a value of −60 kcal e⁻¹.
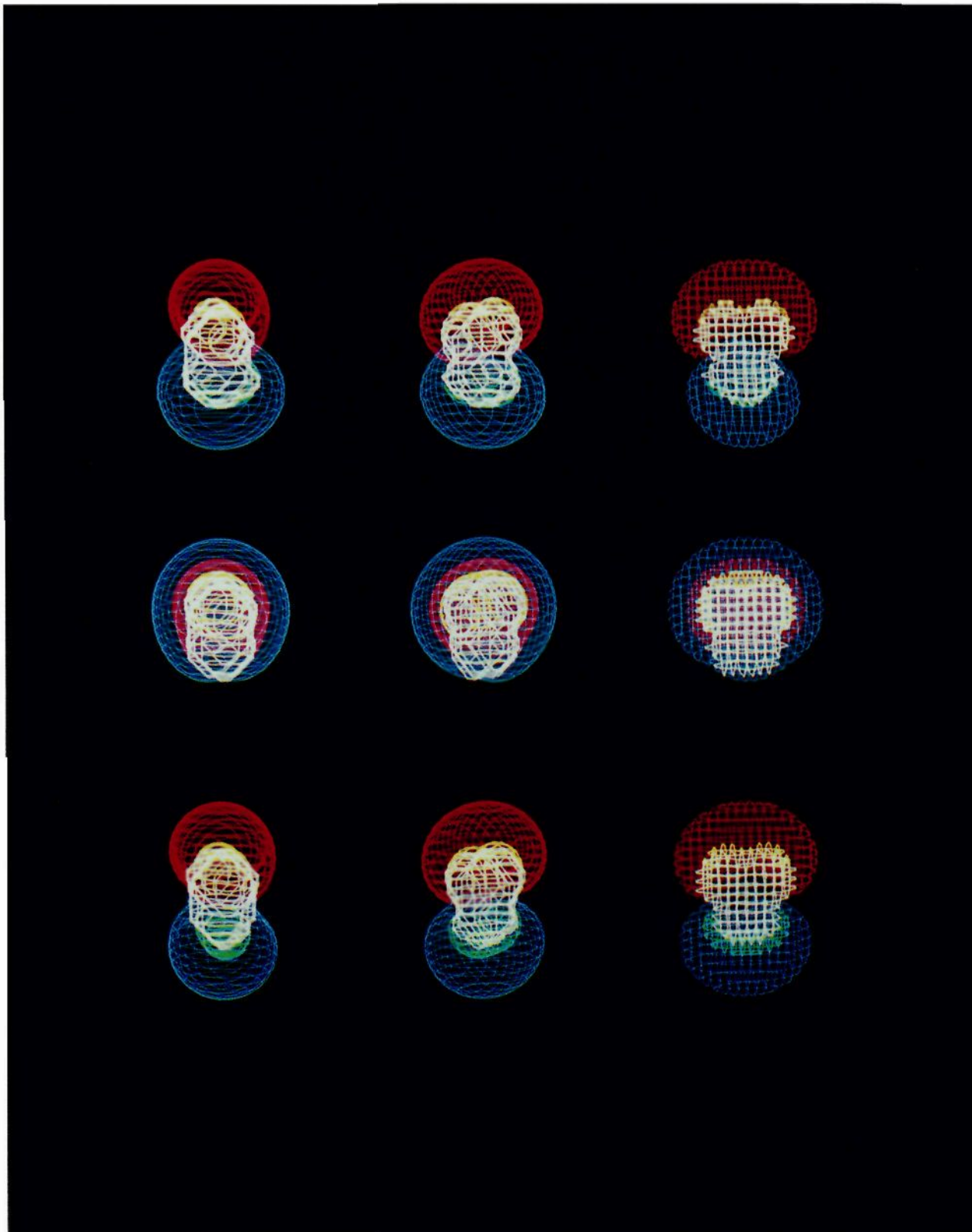
Figure 13. Sequence 1, top: Three-dimensional perspective chicken-wire plots of the electrostatic potential for nitromethane as viewed from three different angles about the C–N internuclear axis proceeding left to right across the page. The molecules are oriented such that the nitro group is toward the top of the page. Constant potential surfaces are represented by red (-10 kcal e^{-1}), blue ($+10$ kcal e^{-1}), yellow (-30 kcal e^{-1}), and green ($+30$ kcal e^{-1}) contours. The white contours form a molecular surface as defined by van der Waals distances. Sequence 2, middle: Three-dimensional perspective chicken-wire plots of the electrostatic potential for nitromethide as viewed from three different angles about the C–N internuclear axis proceeding left to right across the page. Constant potential surfaces are represented by blue (-80 kcal e^{-1}), red (-110 kcal e^{-1}), and yellow (-140 kcal e^{-1}) contours. White contours and orientation are as in sequence 1. Sequence 3, bottom: Three-dimensional perspective chicken-wire plots of the electrostatic potential for nitramide as viewed from three different angles about the N–N internuclear axis proceeding left to right across the page. Contours and orientation are as in sequence 1.

Table I. Optimized Geometrical Parameters and Energies for AB–NO$_2$ Obtained with the 3-21G Basis Set[d]

	A = C B = H$_3$ C_s	A = C$^-$ B = H$_2$ C_{2v}	A = N B = H$_2$ C_{2v}
energy	−242.25585	−241.66332	−258.13793
R(A–N)	1.492 (1.481)[a]	1.295	1.354 (1.427)[b]
R(N–O)	1.240 (1.209, 1.223)[a]	1.346	1.248 (1.206, assumed)[b]
R(A–H)	1.080 (1.098)[a]	1.066	0.994
R(A–H′)	1.074		
∠HAN	107.0 (107.3)[a]	118.7	116.2[c]
∠H′AN	107.2 (107.3)[a]		
∠ANO	116.9 (117.8, 118.9)[a]	119.7	116.4 (114.9)[b]

[a] Reference 12. [b] Reference 13a. [c] In the gas phase, the angle between the NH$_2$ and N–NO$_2$ planes is 51.8°.[13a] [d] Distances, angles, and energies are in angstroms, degrees, and atomic units, respectively. Experimental values are in parentheses.

Table II. Calculated Parameters for the 0.002 e/au^3 Constant Electron Density Surface for CH$_3$NO$_2$, CH$_2$NO$_2^-$, and NH$_2$NO$_2$[d]

	CH$_3$NO$_2$	CH$_2$NO$_2^-$	NH$_2$NO$_2$
electron population	31.794	31.797	31.840
enclosed vol, Å^3	55.0 (~50.6)[a]	55.7 (47.7)[b,c]	48.4 (45.4)[a]
surface area. Å^2	77.1 (~77.5)[a]	77.4 (73.2)[b,c]	70.1 (64.1)[a]
closest approach (Å) to			
C	1.70 (1.70)	1.77 (1.77)[b,c]	
N	1.62 (1.55)	1.62 (1.55)	1.61 (1.55, of NO$_2$) 1.63 (1.55, of NH$_2$)
O	1.48 (1.50)	1.47 (1.50)[c]	1.47 (1.50)
H	1.12 (1.20)	1.17 (1.20)[c]	1.00

[a] Using group increments appropriate for H$_3$–C–(C) and H$_2$N–(C). [b] If this carbon were considered sp^2 hybridized. [c] These values are most appropriate for neutral species of CH$_2$ and NO$_2$. [d] Bondi's values[2c] for van der Waals spheres are shown in parentheses.

the neighborhood of q to obtain FX$_{kl}(q)$, as shown in eq 5.

$$\bar{F}X_{kl}(q) = \frac{1}{N}\sum_{i=1}^{N}FX_{kl}\left(q + \frac{2i - N - 1}{2}\frac{(\Delta)}{N}\right) \qquad (5)$$

Substituting $\bar{F}X_{kl}(q)$ for FX$_{kl}(q)$ in eq 2 yields $\bar{p}(x,y,z)$, which is suitable for obtaining quantitative electron populations. As a result of the averaging procedure, the electron density, $\bar{p}(x,y,z)$, is an averaged density surrounding a grid point. To achieve total electron populations per unit of volume with a precision of at worst 10^{-5} for the elements of hydrogen to neon, N is set equal to 64 and Δ is 0.2 au.

Calculation of van der Waals Parameters. To calculate the volume enclosed by a given constant electron density surface, ρ_{crit}, the number of grid points with $\bar{p}$ greater than or equal to ρ_{crit} are counted and, after the entire grid has been evaluated, multiplied by Δ^3. Electron populations enclosed by a given constant electron density surface are calculated by adding all $\bar{p}$ greater than or equal to ρ_{crit} and multiplying the final sum by Δ^3. Surface areas are calculated by finding from linear interpolation the points of intersection of a constant electron density surface with the edges of a cube, the corners of which are the grid points, and then approximating the surface of intersection as a series of adjacent triangles. The area of any one triangle is calculated by taking half the cross-product of vectors forming two of its sides. The distance of closest approach to the molecule's atoms by a constant electron density surface is determined from the points of intersection of the aforementioned cube. By using these methods with a step size of 0.2 au, values of the volume, surface area, and distances of closest approach are obtained to within 0.5% of rigorous values on spherical systems. The electron population is converged to at worst 10^{-3}e.

Atom-Centered Multipole Expansions. Following Hirshfeld, the promolecule is constructed by superposing spherically averaged atomic $\bar{p}$'s obtained from eq 2 (with use of $\bar{F}(q)$, $N = 64$, and Δ

Table III. Atom-Centered Electric Moments for Nitromethane, Nitromethide, and Nitramide[a]

CH$_3$- NO$_2$	C	N	O (at −z)	H (at z = 0)	H (at −z)
q	−0.012 (−0.38)	0.299 (0.34)	−0.246 (−0.40)	0.073 (0.28)	0.066 (0.27)
μ_{100}	0.034	−0.011	−0.163	−0.066	−0.069
μ_{010}	0.009	0.003	−0.010	0.158	−0.077
μ_{001}	0	0	0.258	0	0.134
μ_{200}	−3.938	−3.800	−3.829	−0.683	−0.706
μ_{110}	0.002	−0.005	0.000	0.019	−0.011
μ_{101}	0	0	−0.152	0	0.005
μ_{020}	−4.160	−3.557	−3.736	−0.741	−0.714
μ_{011}	0	0	−0.005	0	0.017
μ_{002}	−4.201	−3.788	−3.613	−0.700	−0.744
μ_{300}	−0.965	−0.014	−0.454	−0.246	−0.286
μ_{210}	0.008	0.001	−0.009	0.137	−0.068
μ_{201}	0	0	0.107	0	0.088
μ_{120}	0.064	−0.181	−0.122	−0.081	−0.074
μ_{111}	0	0	−0.007	0	0.002
μ_{102}	−0.024	−0.275	0.071	−0.073	−0.096
μ_{030}	−0.260	0.005	−0.009	0.535	−0.247
μ_{021}	0	0	0.153	0	0.147
μ_{012}	0.282	−0.004	0.002	0.168	−0.094
μ_{003}	0	0	0.291	0	0.439

CH$_2$- NO$_2^-$	C	N	O (at −z)	H (at −z)
q	−0.204 (−0.212)	0.174 (0.104)	−0.489 (−0.595)	+0.004 (+0.149)
μ_{100}	0.056	0.057	−0.185	−0.088
μ_{001}	0	0	0.267	−0.130
μ_{200}	−4.391	−4.042	−4.018	−0.778
μ_{101}	0	0	−0.246	−0.016
μ_{020}	−4.812	−3.841	−4.149	−0.858
μ_{002}	−4.536	−3.866	−3.761	−0.818
μ_{300}	−0.700	0.107	−0.493	−0.324
μ_{201}	0	0	0.095	−0.097
μ_{120}	−0.126	0.008	−0.158	−0.120
μ_{102}	0.157	−0.256	0.054	−0.128
μ_{021}	0	0	0.195	−0.175
μ_{003}	0	0	0.333	−0.429

NH$_2$- NO$_2$	N (of NH$_2$)	N (of NO$_2$)	O (at −z)	H (at −z)
q	−0.144 (−0.559)	0.345 (0.548)	−0.267 (−0.404)	0.167 (+0.439)
μ_{100}	0.084	−0.038	−0.154	−0.126
μ_{001}	0	0	0.248	−0.195
μ_{200}	−3.578	−3.808	−3.824	−0.636
μ_{101}	0	0	−0.171	−0.012
μ_{020}	−4.139	−3.655	−3.809	−0.691
μ_{002}	−3.766	−3.795	−3.600	−0.661
μ_{300}	−0.462	0.027	−0.434	−0.464
μ_{201}	0	0	0.098	−0.135
μ_{120}	−0.032	−0.043	−0.110	−0.169
μ_{102}	0.122	−0.288	0.071	−0.159
μ_{021}	0	0	0.161	−0.269
μ_{003}	0	0	0.270	−0.592

[a] All moments are in atomic units and are expressed as the charge (q), first ($i + j + k = 1$), second ($i + j + k = 2$), ..., etc., electric moments. The coordinate system is that used in the figures. Dipoles point from minus to plus, i.e., −→−→−→+. For comparison, Mulliken charges are shown in parentheses after the Hirshfeld charge.

= 0.2 au). The total density at any point is then divided among the atoms of the molecule in the same proportions as the corresponding spherically averaged atoms contribute density to the promolecule. Atom-centered electric moments are then obtained by rectangular integration over Cartesian coordinates as shown in eq 6.

$$\mu_{p,q,r}^{atom} = \Delta^3\sum_{ijk}x_{atom}^{p}y_{atom}^{q}z_{atom}^{r}\bar{p}_{atom}(x_i,y_j,z_k) \qquad (6)$$

On the right-hand side of eq 6, the atom subscript indicates that atom-centered coordinates and the appropriate atom-associated charge densities in the molecule (which are taken as negative to obtain negative charges upon multiplication of ρ by a volume)

are to be used. The atom-centered electric moments obtained from eq 6 are then used to calculate the usual electric multipole moments. In the current notation, charges (q) are obtained by adding the nuclear charge to μ_{000}, μ_{010} is the y component of the dipole or first electric moment, μ_{110} is the xy component of the second electric moment tensor, etc.

With use of these procedures, convergence to better than 0.5% is obtained for the individual multipole moments.

Electrostatic Potential. With the multipole expansions in hand, the electrostatic potential, which is numerically equal to the electrostatic energy of a unipositive point charge at any position, can be readily calculated by using the formulas of Rein[7] and Buckingham.[8] This method of calculation allows the potential to be generated routinely on a three-dimensional grid once the multipoles have been obtained. Other advantages arise because the multipole expansion is an inverse power series in R; hence, it is easily differentiable. This will alow for the rapid calculation of the force resulting from the potential.[9] On the other hand though, the potential calculated in this fashion is only valid if the atoms of the molecule are not approached much more closely than their van der Waals radii.

Test calculations indicate that the procedure in eq 6 yields an electrostatic energy for a unipositive point charge converged to within 1 kcal.

Graphics. In addition to the usual two-dimensional representations, multicolor chicken-wire plots were produced to illustrate the three-dimensional featues of the electrostatic potential, using the programs WDIF[10] and WDIZ.[11] WDIZ will produce movies, which helps enable the visualization of features in three-dimensional space without the removal of hidden lines. The sequences appearing in this paper are selected frames from such movies (Figure 13).

Results and Discussion

SCF Calculations. The geometries and energies obtained from the SCF calculations for nitromethane, nitromethide, and nitramide are presented in Table I. For nitromethane, the C_s conformation corresponding to that found experimentally[12] was fixed, but all other parameters were optimized; for other molecules, C_{2v} structures were predicted to be minima, as verified by force constant calculations. In general, the agreement of theoretical and experimental geometries is about what can be expected at this level of theory. Bothersome though is the prediction of a planar structure for nitramide, when this molecule is known to be nonplanar by 51° in the gas phase.[13a] The barrier to inversion, however, is believed to be very small (probably significantly less than 3 kcal), and the calculations indicated that there is little energetic consequence of bending the hydrogens out of plane. Since most other nitramines are planar, and indeed nitramide is planar in the solid phase,[13b] use of a planar nitramide seems acceptable.

Electron Density Calculations. The results from the quantitative analysis of the electron distributions calculated according to eq 1–5 are shown in Table II. In keeping with the idea that the 0.002 e/au³ constant electron density surface constitutes a molecular surface,[14,15] a very high proportion of the total charge is enclosed: 99.4%, 99.4%, and 99.5% for CH_3NO_2, $CH_2NO_2^-$, and NH_2NO_2,

respectively. The concept is further corroborated by comparing the volume, surface area, and distances of closest approach calculated from the ab initio electron densities and standard van der Waals parameters.[2c]

Density Deformation Maps. Density deformation maps are created by subtracting from the electron density of the molecule the electron density of the promolecule. Figures 1–3 illustrate this quantity in a plane for the subject molecules. The deformation maps show regions of negative deformation in the N–O bonds of the nitro group and the N–N bond in nitramide. Negative deformations along N–O bonds qualitatively similar to those calculated here have been observed experimentally[16,17] and have been the subject of much discussion.[18–22] These calculations strongly confirm the presence of negative deformations along N–O and N–N bonds, although their interpretation remains clouded.

Positive deformations are found along the X–H (X = C, N) bonds in all three cases, though the deformation is not peaked in the vicinity of the bond midpoint. Thus, as illustrated in Figures 1–3, the maximum deformation along the X–H bond lies on the hydrogen atom. Interestingly, deformations in the very near vicinity of the carbon and nitrogen nuclei are negative and most negative at the nucleus. Deformations at the oxygen nuclei are almost zero, but they become negative along the N–O bond direction (both in front of and behind the nucleus). Deformations near the heavy-atom nuclei have been left out of the figures, because the contours would be too close together and, thus, unintelligible. Lone pairs of electrons are also distinguished by positive deformations on the oxygens of the nitro group in all three molecules. Experimentally, similar features of the nitro group have been found.[16,17] Nitromethide does not exhibit a lone pair on carbon, and large, noncylindrical, positive deformations are apparent in the C–N bond. Both these features suggest that the C–N bond should be regarded as a double bond. In contrast, the NH_2 lone pair in nitramide is quite apparent, suggesting a lack of double-bond character in the N–N bond.

Atom-Centered Multipole Expansions. The electric moments obtained from eq 6 for nitromethane, nitromethide, and nitramide are given in Table III. For comparison, Mulliken charges are also included in Table III.

From Table III, it is apparent that the Hirshfeld charges show the least variation from molecule to molecule. Comparing nitromethane and nitramide reveals that, for example, the Hirshfeld charge of the nitro group nitrogen changes only 0.05, while the Mulliken charge changes by 0.21. The similarity of the Hirshfeld charges and of the higher moments for the nitro group in these two molecules indicates that, although attached to two very different substituents, the electronic structure of the nitro group remains in large part the same. This is, of course, just why group additivity schemes and functional group analysis are useful and suggests that group multipole expansions may be derived and reliably used. In this connection, it would be best to obtain the group parameters from as large and accurate a calculation as possible. Once a set of parameters were obtained, however, they could be very widely used.

Determining Expansions. Previous studies have shown that

(7) (a) Rein, R. *Adv. Quantum Chem.* **1973**, *7*, 335–396. (b) Rein, R. In "Electronic Structure of Polymers and Molecular Crystals"; Andie J. M., Ladik, J., Delhalle, J. Eds.; Plenum Press: New York, 1975; pp 505–545.

(8) Buckingham, A. D. In "Intermolecular Interactions: From Diatomics to Biopolymers"; Pullman, B., Ed.; John Wiley & Sons: New York, 1978; Chapter 1.

(9) Dovesi, R.; Pisani, C.; Ricca, F.; Roetti, C. *J. Chem. Soc., Faraday Trans. 2* **1974**, *70*, 1381–1388.

(10) The author wishes to thank J. Kershner for allowing the use of his program.

(11) The author wishes to thank B. Holian and R. Hotchkiss for allowing the use of their program.

(12) Trevino, S. F.; Prince, E.; Hubbard, C. R. *J. Chem. Phys.* **1980**, *73*, 2996–3000.

(13) (a) Tyler, J. K. *J. Mol. Spectrosc.* **1963**, *11*, 39–46. (b) Beevers, C. A.; Trotman-Dickenson, A. F. *Acta Crystallogr.* **1957**, *10*, 34–36.

(14) Francl, M. M.; Hout, R. F., Jr.; Hehre, W. J. *J. Am. Chem. Soc.* **1984**, *106*, 563–570.

(15) (a) Bader, R. F. W.; Henneker, W. H.; Cade, P. E. *J. Chem. Phys.* **1967**, *46*, 3341–3363. (b) Bader, R. F. W.; Beddall, P. M.; Cade, P. E. *J. Am. Chem. Soc.* **1971**, *93*, 3095–3107.

(16) (a) Wang, Y.; Blessing, R. H.; Ross, F. K.; Coppens, P. *Acta Crystallogr., Sect. B* **1976**, *32*, 572–578. (b) Coppens, P.; Lehmann, M. S. *Acta Crystallogr., Sect. B* **1976**, *32*, 1777–1784.

(17) Ryan, R.; Cromer, D.; Wasserman, H., private communication to the author concerning the electron density distribution of nitroguanidine and various picrate salts.

(18) Dunitz, J. D.; Seiler, P. *J. Am. Chem. Soc.* **1983**, *105*, 7056–7058.

(19) Heijser, W.; Baerends, E. J.; Ros, P. *J. Mol. Struct.* **1980**, *63*, 109–120.

(20) Bader, R. F. W. In "The Force Concept in Chemistry"; Deb, B. M., Ed.; Van Nostrand Reinhold: Dallas, 1981; Chapter 2, Section 2–3 and references therein.

(21) Rosenfeld, J. L. *J. Acta Chem. Scand.* **1964**, *18*, 1719–1738.

(22) Ransil, B. J.; Sinai, J. J. *J. Chem. Phys.* **1967**, *46*, 4050–4074.

multicentered expansions of various types are useful for calculating electrostatic properties associated with a single molecule[3,9,23,24] or for a collection of molecules.[24,25] Multicentered multipole expansions derived directly from the electron distribution are no exception and are probably superior to those obtained from the overlap population of basis functions in that the latter are likely to share many of the known deficiencies of the Mulliken analysis. Multipole expansions reasonably approximate the potential calculated in a rigorous fashion subject to a few constraints that are discussed below.

In deriving the expansions, if the charge distribution of the molecule is truncated too soon, significant errors occur. Because the 0.002 e/au^3 was found to correspond in a fashion to the molecular surface, it might be concluded that in calculating the electric moments, only the electron density within this contour needs to be considered. This is false. Calculations considering only the charge included within the 0.002 contour compared with calculations considering the charge contained in a box, the sides of which come no closer than 4 to 5 au of any atom in the molecule, reveal discrepancies in the potential of up to 15 kcal e^{-1}. It was found that the box described above will normally include to within 1×10^{-4} all the electrons in the molecule and will yield satisfactory results in the cases studied.

A second issue arises in truncating the multipole expansion. This problem was studied by calculating separately potential contributions of the dipole, quadrupole, octopole, and hexadecapole moments. Thus, Figures 4–6 (A) show the dipole contribution, Figures 4–6 (B) show the quadrupole contribution, Figures 4–6 (C) show the octopole contribution, and Figures 4–6 (D) show the hexadecapole contribution to the potential for each of the test molecules. Figures 4–6 (D) illustrate that the expansions yield a potential converged to within about 1 kcal e^{-1} after consideration of octopole moments, provided that the atoms of the molecule are not approached more closely than their van der Waals radii. Within this distance, the accuracy of the expansion rapidly degrades.

Figures 7–9 show the differences between the potential calculated rigorously and that calculated with the use of multipole expansions. Regions within the van der Waals distance[2c] of the atoms are blanked out, because it is within these regions that very large errors resulting from the multipole expansions occur. Also, the multipole expansions give a potential too small by as much as 1–10 kcal e^{-1} at distances from the atoms ranging from about 2.0 Å to their van der Waals radii. These errors indicate that the multipole expansions systematically give a potential numerically too small. Only in the lone-pair region of the NH_2 nitrogen in nitramide does the multipole expansion yield a potential too large and then only by about 1.5 kcal e^{-1}.

Electrostatic Potentials. Three-dimensional perspective plots of the electrostatic potential are shown in sequences 1–3 in Figure 13 and in more standard two-dimensional representations in Figures 10–12. It is interesting to note that the methyl group of nitromethane is associated with strictly positive potentials. This contrasts with the negative potentials found near the methyl groups of methane,[26] ethane,[26] and acetamide.[27] It is likely that this feature is not present in nitromethane because of the electron-withdrawing effect of the nitro group. A similar effect has been noted for acetonitrile and acetic acid.[28] Additionally, it is known that nitro group substitution in cyclopropane causes negative potentials associated with bent bonds to become positive.[29]

The potential about nitromethide (sequence 2 (Figure 13) and Figure 11) is everywhere negative as indicated in the illustrations. There appears no noticeable lone pair of electrons on carbon that might be associated with the formation of the anion and the most negative potential occurs along the C_2 axis between the two oxygens of the nitro group.

In nitramide, the nitro group appears very similar to that in nitromethane, although its potential is slightly more negative than that in nitromethane. Also noticeable are regions more positive about hydrogen in nitramide than in nitromethane. There is no negative potential associated with the NH_2 nitrogen lone pair that is clearly visible in Figure 3; the potential reaches a minimum value of about +4 kcal e^{-1} in this region as shown in Figure 12. Normally, of course, for a simple amine, negative regions would be found near the lone pair.[30]

Conclusion. A fast and efficient method for calculating the electron density distribution has been implemented that allows the quantitative integration of the electron density function over arbitrary regions of three-dimensional space. Parameters associated with the 0.002 e/au^3 constant electron density surface, such as electron population, volume, surface area, and distances of closest approach to the atoms of the molecule, were calculated and shown to support the concept of the 0.002 e/au^3 constant electron density surface as a "molecular" surface. Density deformation maps were found to be in qualitative agreement with experiments showing negative deformations along the N–O bond of a nitro group. Finally, multipole expansions were derived and shown to approximate reasonably the electrostatic properties of nitromethane, nitromethide, and nitramide.

(23) Pack, G. R.; Wang, H.; Rein, R. *Chem. Phys. Lett.* **1972**, *17*, 381–384 and references therein.

(24) For an in-depth discussion of this topic, see: Claverie, P. In "Intermolecular Interactions: From Diatomics to Biopolymers"; Pullman, B., Ed.; John Wiley & Sons: New York, 1978; Chapter 2, but especially Section V, Subsect A and B.

(25) For discussion of an interesting application, see: Buckingham, A. D.; Fowler, P. W. *J. Chem. Phys.* **1983**, *79*, 6426–6428. For a critque, see: Baiocchi, B. A.; Reiker, W.; Klemperer, W. *J. Chem. Phys.* **1983**, *79*, 6428–6429.

(26) Politzer, P.; Daiker, K. C. *Chem. Phys. Lett.* **1975**, *34*, 294–297.

(27) Orita, Y.; Pullman, A. *Theor. Chim. Acta* **1977**, *46*, 251–258.

(28) Politzer, P.; Daiker, K. C. In "The Force Concept in Chemistry"; Deb, B. M., Ed.; Van Nostrand Reinhold: Dallas, 1981; pp 354–356.

(29) Politzer, P.; Domelsmith, L. N.; Sjöberg, P. *Chem. Phys. Lett.* **1982**, *92*, 366–370.

(30) Pullman, A. In "Chemical and Biochemical Reactivity"; Bergmann, E. D., Pullman, B., Eds.; D. Reidel: Dordrecht, Holland, 1974; pp 1–11.